Numerical Analysis of Ponded Infiltration Experiment under Different Experimental Conditions

Jaromír DUŠEK, Michal DOHNAL and Tomáš VOGEL

Department of Hydraulics and Hydrology, Faculty of Civil Engineering, Czech Technical University in Prague, Prague, Czech Republic

Abstract: One of the most important properties, affecting the flow regime in the soil profile, is the topsoil saturated hydraulic conductivity (K_s). The laboratory-determined K_s often fails to characterise properly the respective field value; the K_s lab estimation requires labour intensive sampling and fixing procedures, difficult to follow in highly structured and stony soils. Thus, simple single- or double-ring ponded infiltration experiments are frequently performed in situ to obtain the field scale information required. In the present study, several important factors, affecting the infiltration rate during the infiltration experiments, are analysed using three-dimensional axisymmetric finite-element model S2D. The examined factors include: (1) the diameter of the infiltration ring, (2) the depth of water in the ring, (3) the depth of the ring insertion under the soil surface, (4) the size and the shape of the finite-element mesh near the ring wall, and (5) the double- vs. single-ring setup. The analysis suggests that the depth of the ring insertion significantly influences the infiltration rate. The simulated infiltration rates also exhibit high sensitivity to the shape of the finite-element mesh near the ring wall. The steady-state infiltration rate, even when considering a double-ring experiment, is significantly higher than the topsoil saturated hydraulic conductivity. The change of the water depth in the outer ring has only a small impact on the infiltration rate in the inner ring.

Keywords: infiltration; single-ring infiltrometer; saturated hydraulic conductivity; depth of insertion; ponding depth; soil hydraulic properties; three-dimensional axisymmetric flow

The topsoil saturated hydraulic conductivity (K_s) is one of the most important properties affecting the flow regime in the soil profile. The laboratory-determined K_s often fails to characterise properly the respective field value; the K_s lab estimation requires labour intensive sampling and fixing procedures, difficult to follow in highly structured and stony soils. Thus simple double- or single-ring ponded infiltration experiments are frequently performed in situ to obtain the field scale information required.

The infiltration experiment may be performed using mini-disk infiltrometers, with adjustable capillary pressure, or ring infiltrometers, to establish the ponded conditions. The localised water supply from both types of infiltrometer inevitably causes a three-dimensional character of flow under the circular source. At the beginning of the infiltration experiment, capillary forces dominate. As the infiltration rate approaches a quasi steady-state condition, the gravity forces become also important.

Supported by the Czech Science Foundation, Project No. 526/08/1016 and by the Ministry of Environment of the Czech Republic, Project No. SP/2e7/229/07.

From the disk steady-state infiltration rate it is possible to determine the hydraulic conductivity using analytical solution (Ankeny *et al.* 1991). Transient infiltration data can be used as well to accomplish this goal; however the inverse procedures must be invoked (e.g. Ramos *et al.* 2006). The inverse analysis was used to obtain K_s from a field ponded infiltration experiment e.g. by Vogel and Císlerová (1993).

Recently, several studies on the geometrical setup of single- or double-ring infiltration experiments (e.g. the depth of water in the ring, the ring diameter and the ring insertion) were published. Chowdary *et al.* (2006) analysed in situ the geometrical setup of the infiltration aiming at a proper design and management of field irrigation systems. Three-dimensional numerical studies of the field infiltration experiments were carried out by e.g. Reynolds and Elrick (1990) and Wu and Pan (1997). Wu and Pan (1997) attempted to develop a generalised infiltration solution and evaluated the respective geometrical effect on the infiltration curve. Reynolds and Elrick (1990) defined an effective shape factor which assesses the geometrical setup of the infiltration experiment; in their study, the shape factor was used to calculate the field K_s. Numerical studies of the infiltration experiment were also conducted by e.g. Šimůnek (1988) and Touma *et al.* (2007).

The objective of this paper is to evaluate numerically different factors that determine the infiltration rates during the field infiltration experiments and the resulting values of the saturated hydraulic conductivity. The analysed factors include: (1) the diameter of the infiltration ring, (2) the depth of water in the ring, (3) the depth of the ring insertion under the soil surface, (4) the size and shape of the finite-element mesh near the ring wall, and (5) the double- vs. single-ring setup. The individual and combined effects were analysed in detail by means of three-dimensional axisymmetric simulations carried out by two-dimensional numerical model S2D (Vogel *et al.* 2000).

MATERIALS AND METHODS

The mathematical modelling involved three-dimensional axisymmetric simulations carried out by the two-dimensional code S2D. To parameterise the unsaturated hydraulic conductivity function, modified Mualem-van Genuchten approach was used (Vogel *et al.* 2001).

The governing partial differential equation (Richards' equation) was assumed in the following form

$$C\frac{\partial h}{\partial t} = \nabla \cdot (K\nabla h) + \nabla \cdot (K\nabla z) \quad (1)$$

where:

h – soil water pressure head (L)

K – hydraulic conductivity tensor (L/T)

C – specific capacity (1/L)

z – vertical coordination oriented upward (L)

t – time (T)

The conductivity tensor was assumed to be isotropic, i.e. the conductivity is defined at any particular location and time by a single scalar value.

Table 1 shows the soil hydraulic parameters of coarse sandy loam used for the numerical experiments. In this study, we assumed a homogeneous soil profile. The soil characteristics are based on the soil samples taken from the soil profile of Dystric Cambisol in the Volynka river watershed, Sumava Mountains, Southern Bohemia (Císlerová *et al.* 1988).

As the initial condition, soil water pressure head was set equal to –1000 cm in the entire flow domain. The two-dimensional finite-element mesh (see Figure 6) rotates along the central axis of the infiltration ring, thus creating three-dimensional axisymmetric domain with dimensions of 200 × 150 cm. The vertical dimension of the flow domain was chosen to be large enough to meet the requirement that the lower boundary does not affect the infiltration rate on the soil surface. A Dirichlet boundary condition with the prescribed value of the pressure head was used for the flooded area of the infiltration ring. The lower boundary was treated as a unit hydraulic gradient boundary.

Table 1. Parameters of soil hydraulic properties (modified Mualem-van Genuchten parameterisation)

Depth (cm)	θ_r (–)	θ_s (–)	h_s (cm)	α (1/cm)	n (–)	K_s (cm/h)
0÷150	0.01	0.461	–3.42	0.083	1.111	5.0

All other parts of the flow domain boundary were assumed to be impermeable.

The geometry of a single-ring infiltration experiment is depicted in Figure 1. In a series of three subsequent simulation runs, the diameter of the infiltration ring varied from 35.7 cm to infinity (D = 35.7, 61.8, ∞). For the simulation run corresponding to the ring diameter of infinite length, one-dimensional code HYDRUS 5.0 (Vogel *et al.* 1996) was used instead of S2D code. The depth of water H in the ring was alternatively assumed to be 0, 5, and 10 cm, respectively. The depth of the ring insertion I under the soil surface was set at 0, 5, 10, and 20 cm, respectively. For the numerical experiments with the double-ring setup, the diameter of the outer ring was 61.8 cm. Finally, the impact of the size and shape of the finite-element mesh near the ring wall was tested by using two different finite-element meshes.

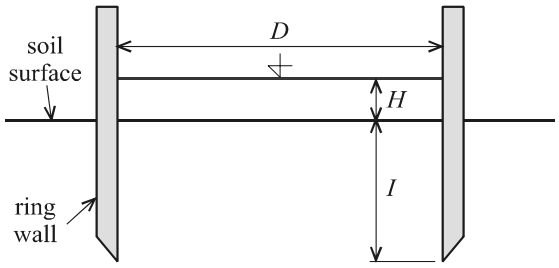

Figure 1. Schematic of the single-ring infiltration experiment; symbol D stands for the diameter of the ring, H for the depth of water in the ring, and I denotes the depth of the ring insertion under the soil surface

RESULTS AND DISCUSSION

Figure 2 illustrates the effect of changing the diameter of the infiltration ring by showing the infiltration rate vs. time throughout the infiltration experiment. Note that the one-dimensional simulation rates (marked as D = ∞ in Figure 2) approach asymptotically the value of the saturated hydraulic conductivity. For the three-dimensional scenarios, the steady-state infiltration rate is higher than K_s. This is caused by the three-dimensional character of the wetting front. The smaller the diameter of the ring, the higher the steady-state infiltration rate. By increasing further the ring diameter, the 3D simulation results will converge to the D = ∞ infiltration curve. A similar trend in the infiltration rates in response to varying D has been also predicted for other combinations of the water depth H and ring insertion I (not shown in this paper).

In Figure 3, the effect of varying the depth of water H in the ring is shown. From the figure it seems obvious that a higher water level maintained in the ring produces higher infiltration rates due to a greater pressure gradient. Again, a similar trend in the infiltration rates in response to varying H is simulated for other combinations of D and I (not shown here).

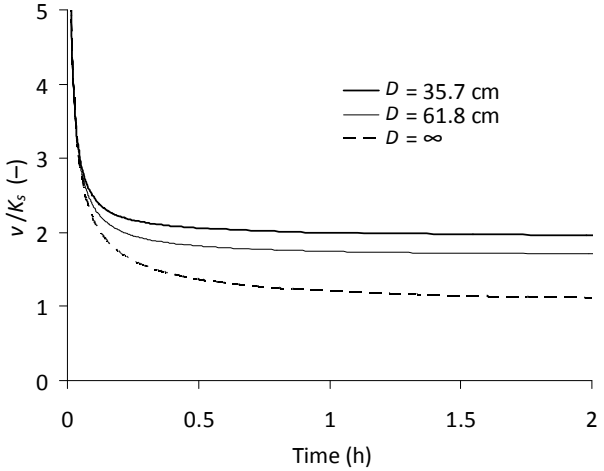

Figure 2. The effect of changing the ring diameter D; the depth of water in the ring H = 5 cm, the depth of the ring insertion I = 5 cm; the ring diameter of infinite length corresponds to one-dimensional water flow simulation (D = ∞)

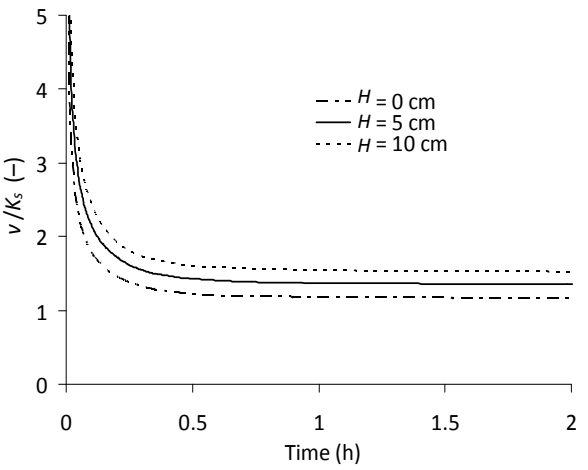

Figure 3. The effect of changing the depth of water H in the ring; the ring diameter D = 61.8 cm, the depth of the ring insertion I = 20 cm

The effect of changing the depth of the ring insertion on the infiltration rate is shown in Figure 4. Substantial deviations among the simulations with different I are predicted. It is evident that, if the ring insertion is not considered in the mathematical modelling of the ponded infiltration, a significant overestimation of the infiltration rate is obtained. For our particular case study, the simulation with zero depth of insertion delivered the steady-state infiltration rate higher than 3 K_s. The effect of the depth of the ring insertion is enhanced for greater depths of water in the ring H. As one can expect, the effect of the insertion depth becomes less important for larger sizes of the infiltration ring (i.e., the infiltration rate at the steady-state was about 2.5 K_s for the simulation with zero depth of insertion, using H = 10 cm and D = 61.8 cm).

The effects of changing the size and shape of the finite-element mesh near the ring wall are shown in Figure 5 and Figure 6. Figure 5 depicts the simulated infiltration rate (for D = 35.7 cm, H = 5 cm, and I = 10 cm) as a function of time for the scenario with two different finite-element meshes. The two simulation scenarios are referred to as wrong mesh and correct mesh, respectively. The correct mesh was constructed from triangular elements of continuously changing sizes, in contrast to the wrong mesh. In addition, the minimum allowed element angle for the correct mesh was specified so that the mesh anisotropy was kept small. As follows from Figure 5, the simulated infiltration rates exhibit a high sensitivity to the shape of the finite-element mesh near the ring wall.

The 2D cross-section of the pressure head field below the ring at t = 20 min is shown in Figure 6.

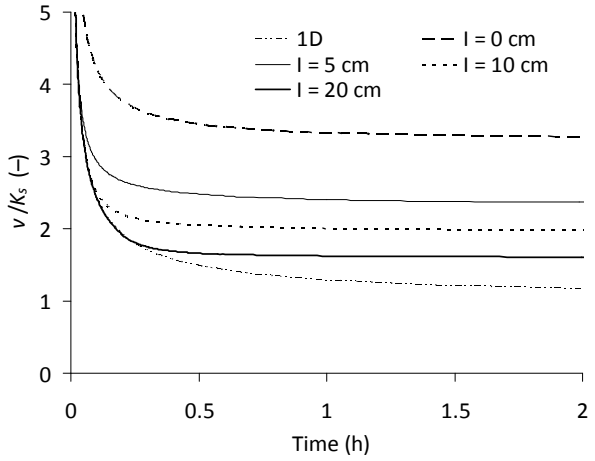

Figure 4. The effect of changing the depth of the ring insertion I; the depth of water in the ring H = 10 cm, the ring diameter D = 35.7 cm

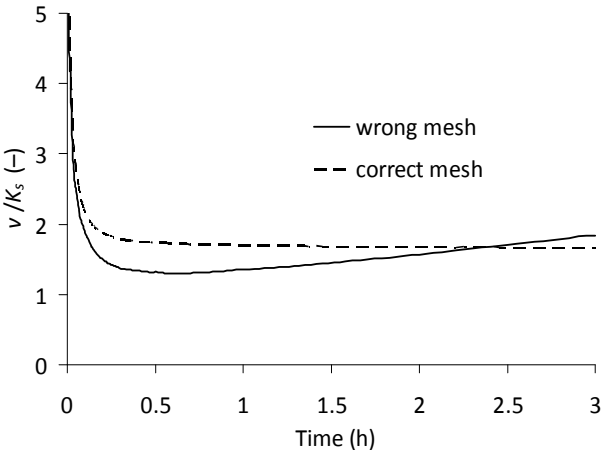

Figure 5. The effect of changing the size and shape of the finite-element mesh near the ring wall; the results for the simulations using wrong and correct computational meshes are shown; scenario with D = 35.7 cm, H = 5 cm, and I = 10 cm

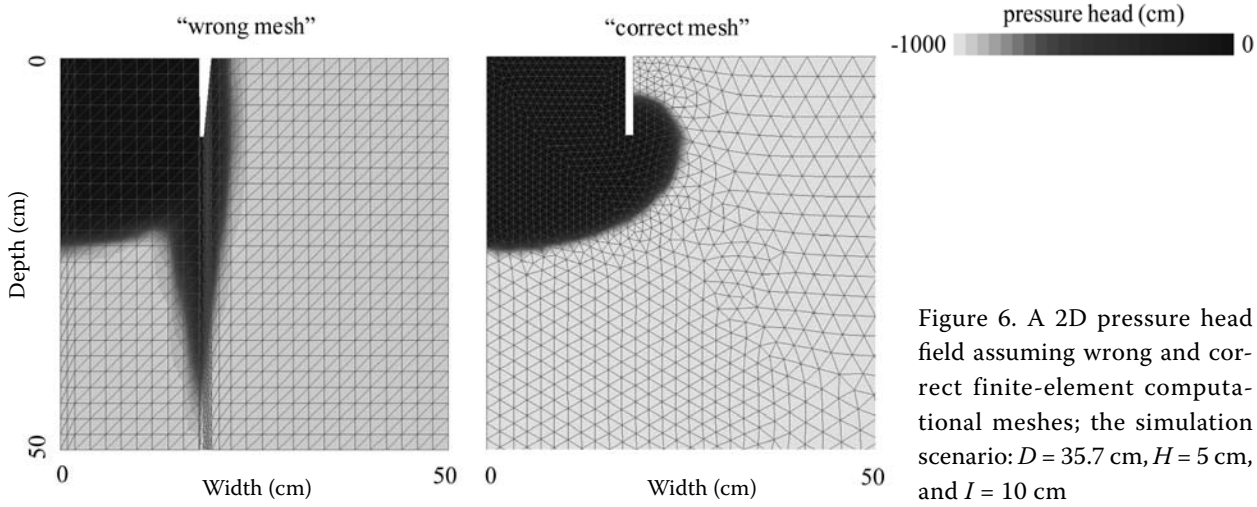

Figure 6. A 2D pressure head field assuming wrong and correct finite-element computational meshes; the simulation scenario: D = 35.7 cm, H = 5 cm, and I = 10 cm

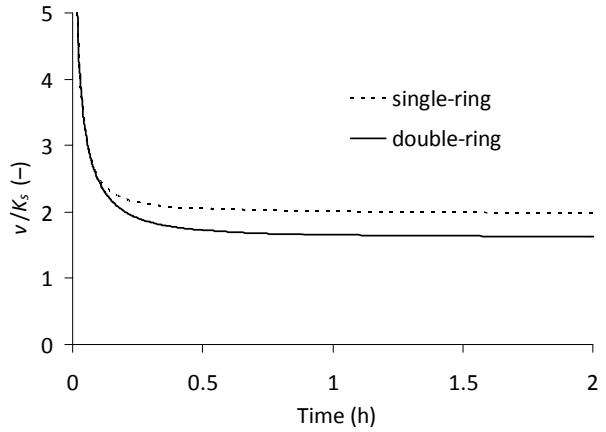

Figure 7. The effect of using double-ring vs. single-ring. The single-ring infiltration rate is compared with the inner ring rate of the double-ring setup; the simulation scenario: D = 35.7 cm, H = 10 cm, and I = 10 cm

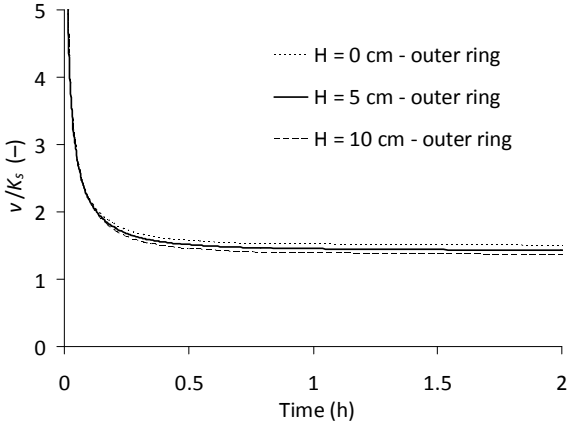

Figure 8. The effect of changing the water depth in the outer ring of the double-ring infiltration experiment. Infiltration rates in the inner ring are shown; the simulation scenario: D = 35.7 cm, H = 5 cm (inner ring), and I = 10 cm

The detail is based on the wrong and correct finite-element meshes, which are shown as well. Note that the computational elements near the ring wall exceed the recommended height-to-width ratio due to the mesh deformation technique used to generate the mesh. The mesh anisotropy induced the development of a finger-like water flow along the ring wall.

The comparison between the infiltration rates in a single-ring infiltrometer (D = 35.7 cm) and in the inner ring of a double-ring infiltrometer, assuming H = 10 cm and I = 10 cm, is depicted in Figure 7 (the outer ring diameter was 61.8 cm). The water flow in the outer ring caused a slight reduction of the infiltration rate in the inner ring. However, it can be seen that even if the double-ring setup is considered, the steady-state infiltration rate is significantly higher than K_s. This implies the well known, but not always fully respected, fact that the double-ring experiment does not deliver directly the value of the saturated hydraulic conductivity, and thus the steady-state infiltration rate cannot be interpreted as K_s. Again, the increase of the water depth in the infiltration ring leads to more pronounced differences between the steady-state infiltration rates for single- and double-ring setups and, as mentioned above, a deeper ring insertion makes the infiltration rate smaller.

In Figure 8, the effect of the water depth in the outer ring of the double-ring setup is examined. The depth of water in the inner ring was kept constant (H = 5 cm) while the water depth in the outer ring was lowered/raised by 5 cm. Such differences seem to be realistic due to the difficulties often encountered during the field double-ring infiltration experiments. The results suggest only a negligible effect of the water depth in the outer ring on the infiltration rate in the inner ring. Note that smaller infiltration rates in the inner ring are predicted for the case of a higher water depth in the outer ring. This is caused by the reduction of the lateral flow component. In this context, it is worth mentioning that the water transfer between the outer and inner rings may be more pronounced in soils with preferential pathways, but such effects are beyond the scope of this study.

CONCLUSIONS

In this study, five important factors were analysed determining the infiltration rate and the water flow regime during the ponded infiltration experiments as well as the subsequent evaluation of the surface hydraulic properties. The factors include: (1) the diameter of the infiltration ring, (2) the depth of water in the ring, (3) the depth of the ring insertion under the soil surface, (4) the size and shape of the finite-element mesh near the ring wall, and (5) the double-ring vs. single ring setup of the experiment.

The results of the numerical study confirm that the effects related to the geometry of the experimental setup significantly influence the water flow in the soil profile. The depth of the ring insertion under the soil surface was found to be the most important geometrical factor. Neglecting the ring insertion in the numerical model may lead to false or biased conclusions, e.g. when the model is used

to verify various methods for the determination of sorptivity and/or hydraulic conductivity. Steady-state infiltration rates, even considering the double-ring experiment, are significantly higher than the saturated hydraulic conductivity. The change of the water depth in the outer ring has only a small impact on the resulting infiltration rates in the inner ring (provided that the preferential flow effects are negligible).

As far as the mathematical modelling of the ponded infiltration experiment is concerned, special attention should be paid to the design of the finite-element mesh and to the proper parameterisation of the soil hydraulic properties near saturation.

References

Ankeny M.D., Mushtaque A., Kaspar T., Horton R. (1991): Simple field method for determining unsaturated hydraulic conductivity. Soil Science Society of American Journal, **55**: 467–470.

Chowdary W.M., Rao M.D., Jaiswal C.S. (2006): Study of infiltration process under different experimental conditions. Agricultural Water Management, **83**: 69–78.

Císlerová M., Šimůnek J., Vogel T. (1988): Changes of steady-state infiltration rates in recurrent ponding infiltration experiments. Journal of Hydrology, **104**: 1–16.

Ramos T.B., Goncalves M.C., Martins J.C., van Genuchten M.Th., Pires F.P. (2006): Estimation of soil hydraulic properties from numerical inversion of tension disk infiltrometer data. Vadose Zone Journal, **5**: 684–696.

Reynolds W.D., Elrick D.E. (1990): Ponded infiltration from a single ring: I. Analysis of steady flow. Soil Science Society of American Journal, **54**: 1233–1241.

Šimůnek J. (1988): Infiltration – numerical simulation. Vodohospodářský časopis, **36**: 407–420. (in Czech)

Touma J., Voltz M., Albergel J. (2007): Determining soil saturated hydraulic conductivity and sorptivity from single ring infiltration tests. European Journal of Soil Science, **58**: 229–238.

Vogel T., Císlerová M. (1993): A scaling-based interpretation of a field infiltration experiment. Journal of Hydrology, **142**: 337–347.

Vogel T., Huang K., Zhang R., van Genuchten M.Th. (1996): The HYDRUS code for simulating One-Dimensional Water Flow, Solute Transport, and Heat Movement in Variably-Saturated Media. Version 5.0 [Research Report No. 140.] U.S. Salinity Lab., ARS, USDA, Riverside.

Vogel T., Gerke H.H., Zhang R., van Genuchten M.Th. (2000): Modelling flow and transport in a two-dimensional dual-permeability system with spatially variable hydraulic properties. Journal of Hydrology, **238**: 78–89.

Vogel T., van Genuchten M.Th., Císlerová M. (2001): Effect of the shape of soil hydraulic functions near saturation on variably-saturated flow predictions. Advances in Water Resources, **24**: 133–144.

Wu L., Pan L. (1997): A generalized solution to infiltration from single-ring infiltrometers by scaling. Soil Science Society of American Journal, **61**: 1318–1322.

Corresponding author:

Ing. Jaromír Dušek, Ph.D., České vysoké učení technické v Praze, Fakulta stavební, katedra hydrauliky a hydrologie, Thákurova 7, 166 29 Praha 6-Dejvice, Česká republika
tel.: + 420 224 354 355, e-mail: jaromir.dusek@fsv.cvut.cz